催化学报
2011 Chinese Journal of Catalysis Vol. 32 No. 6

Article ID: 0253-9837(2011)06-0879-12 **DOI**: 10.1016/S1872-2067(10)60209-4 **Review:** 879–890

Conversion of Solar Energy to Fuels by Inorganic Heterogeneous Systems

Kimfung LI, David MARTIN, Junwang TANG*

Department of Chemical Engineering, University College London, Torrington Place, London, WC1E 7JE, UK

Abstract: Over the last several years, the need to find clean and renewable energy sources has increased rapidly because current fossil fuels will not only eventually be depleted, but their continuous combustion leads to a dramatic increase in the carbon dioxide amount in atmosphere. Utilisation of the Sun's radiation can provide a solution to both problems. Hydrogen fuel can be generated by using solar energy to split water, and liquid fuels can be produced via direct CO_2 photoreduction. This would create an essentially free carbon or at least carbon neutral energy cycle. In this tutorial review, the current progress in fuels' generation directly driven by solar energy is summarised. Fundamental mechanisms are discussed with suggestions for future research.

Key words: solar energy; photocatalysis; carbon dioxide conversion; water splitting

CLC number: O643 **Document code:** A

Received 30 October 2010. Accepted 5 January 2011.

**Corresponding author. Tel: +44-20-7679-7393; E-mail: Junwang.tang@ucl.ac.uk*

This work was supported by the Engineering and Physical Sciences Research Council (EPSRC).

English edition available online at Elsevier ScienceDirect (http://www.sciencedirect.com/science/journal/18722067).

The increasing demand for global energy has drawn much attention to the field of energy development. It is predicted that the annual amount of energy requirement will double in the next fifty years from 13.5 TW/year in 2001 to 27 TW/year in 2050 [1,2]. At present, the main energy output comes from hydrocarbon fuels, and only 20% comes from other energy sources such as tidal power, nuclear energy, biomass, photovoltaics, etc. Hydrocarbon fuels have many advantages over the other types of fuels, including easy storage and transportation, availability and a high volumetric energy density (33 GJ/m^3) [3]. The total amount of global hydrocarbon fuel available is limited and the large amounts of CO_2 emitted from burning hydrocarbon fuels are a significant drawback against their application. Moreover, safety and health issues behind the storage of hydrocarbon fuels are often ignored. The oil spill in the Gulf of Mexico has caused an enormous impact to the marine ecosystem, which has greatly increased the awareness and need for alternative clean energy. Taking into account all these factors, the development of new sources of renewable and clean energy to replace fossil fuels has become one of the most important topics for humans today.

Sunlight is the most abundant renewable energy source in the world. The energy hitting the Earth's surface is about 100000 TW/year [4]. In addition, solar energy is clean, non-monopolized, and environmentally friendly. The only drawback is its intermittent irradiation. Therefore, the ability to capture, convert, and store solar energy for later use is the primary goal for researchers in the field today. Nature has shown us how to utilise sunlight and learning from it will teach us to develop a sustainable energy source. In natural photosynthesis, plants oxidize water in the PSII reaction centre leading to the formation of O_2 and production of reducing equivalents. These are further used in the Calvin cycle in the reduction of CO_2. Following a similar mechanism, an artificial system can be designed not only to oxidize the water in a light driven process to produce O_2 but also to drive the reduction of protons to yield hydrogen. Hydrogen has the highest energy density of fuels by weight. It has a maximum efficiency of 38% when used in an Otto cycle internal combustion engine, which is 8% higher than a gasoline internal combustion engine. Water is the only combustion product of hydrogen driven system. Due to these advantages, hydrogen generation by a sunlight driven water spitting process has been widely investigated.

Besides the concern of the limited amount of hydrocarbon fuels reserve, the impact of burning fossil fuels is huge. Researches based on many climate simulations suggest that at the current increase rate of atmospheric CO_2 concentration, the average global temperature will go up about 6 °C before the end of this century. 6 °C is sufficient to switch Earth's climate from glacial conditions to an ice-free Antarctica [5,6]. While discussions have begun on means to reduce CO_2 emissions, it is apparent that the atmospheric CO_2 concentration will continue to increase due to hydrocarbon consumption. Approximately 1 billion barrels of oil

are consumed to supply the world energy requirement every 12 days, which represents nearly 1 trillion pounds of CO_2 released to the atmosphere. In response to this, there are several strategies developed to reduce CO_2 levels. Reduction of CO_2 levels can be achieved by carbon capture and storage (CCS) in which CO_2 collected from its emission sources would be buried under the Earth [7]. However, the compression and burial of CO_2 require extra energy, generating more CO_2. In addition to the extra energy requirement for storing CO_2, burying CO_2 also has the risk of leakage, and in 1986 the eruption of naturally sequestrated CO_2 asphyxiated 1700 people in Cameroon [8].

Recycling CO_2 and converting it into a high-energy fuel is an advanced solution. However, CO_2 is the thermodynamic final product of combustion, thus it is very stable and CO_2 conversion requires huge energy input. CO_2 can be converted by biomass production process, thermochemical, electrochemical, and photochemical methods. Biomass to fuel is a viable approach for carbon recycling, and involves CO_2 absorption by plants during photosynthesis [9,10]. However, it is well known that the whole process is very time consuming and characterized by an extremely low efficiency. Unlike photoreduction of CO_2, thermal or electrochemical process requires very high temperatures or a strong external voltage bias to provide energy to drive the reaction, which lowers the efficiency of the device and limits its deployment. Photocatalysis can reduce CO_2 to produce hydrocarbons in a similar way to the Calvin cycle in natural photosynthesis. This is also another approach to convert and store solar energy. The following equations ((1)–(8)) illustrate solar fuel generation pathways, including solar H_2 production and conversion of CO_2 to potential fuels driven by photocatalysis [11].

Solar hydrogen:	Chemical potential (eV vs. NHE)	
$2H_2O + 4h^+ \rightarrow O_2 + 4H^+$	1.23	(1)
$2H^+ + 2e^- \rightarrow H_2$	0	(2)
CO_2 conversion:		
$CO_2 + e^- \rightarrow CO_2^-$	–1.49	(3)
$CO_2 + 2H^+ + 2e^- \rightarrow HCOOH$	–0.19	(4)
$CO_2 + 2H^+ + 2e^- \rightarrow CO + H_2O$	–0.19	(5)
$CO_2 + 4H^+ + 4e^- \rightarrow HCHO + H_2O$	–0.06	(6)
$CO_2 + 6H^+ + 6e^- \rightarrow CH_3OH + H_2O$	+0.03	(7)
$CO_2 + 8H^+ + 8e^- \rightarrow CH_4 + H_2O$	+0.18	(8)

This short review focuses on solar hydrogen production from water splitting and CO_2 conversion by inorganic heterogeneous systems and the use of semiconductor photocatalysts. The principles of how inorganic photocatalysts operate under sunlight are first described, and then there is an analysis of the up-to-date research situation including the active materials for both reaction pathways and some important factors influencing conversion efficiency. Finally, mechanistic work that is being carried out to guide the design of the next generation of materials will be discussed.

Photocatalytic fuel production has been widely studied and is a fast moving field. A number of excellent review articles have been published in recent years [11–15]. Therefore, we concentrate on a limited number of representative materials in this tutorial review. We do not consider in detail the use of photocatalytic films as photoanodes and photocathodes and homogeneous systems.

1 Fundamental Knowledge

Water splitting and CO_2 conversion processes share the same energy scheme (Fig. 1). When light is incident on the semiconductor, electrons located in the valence band (VB) in the semiconductor can be excited by light having energy greater than the band gap of semiconductor, the energy difference between the top of the filled valence band and the bottom of the empty conduction band (CB), resulting in the electrons being promoted from the VB to the CB, simultaneously leaving positively charged holes in the VB. The pair can, if recombination does not happen as fast as separation and transportation, travel to the surface of semiconductor and split water to produce oxygen and hydrogen, or reduce CO_2 to yield hydrocarbons (e.g. alcohols)

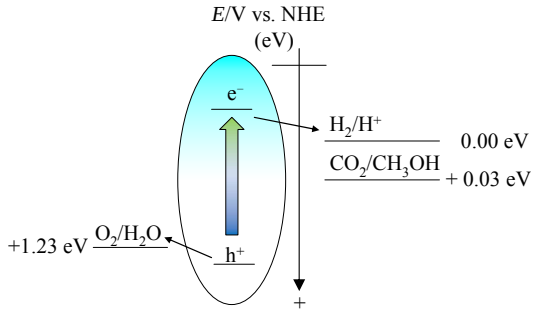

Fig. 1. Systematic diagram of the fundamental mechanism of heterogeneous photocatalysis.

In order to reduce CO_2 to fuel, e.g. methanol, or produce hydrogen from water, the electrons in the CB must have a potential that is more negative than the redox potential of CO_2/CH_3OH (~0.03 eV vs. NHE) or H^+/H_2 (0 eV vs. NHE) to provide the driving force for the reaction. On the other hand, water oxidation occurs when the hole potential is more positive than the redox potential of O_2/H_2O (+1.23 eV vs. NHE). On this basis a minimum band gap energy of 1.23~1.27 eV is required. In practice, the minimum practical energy required to drive photocatalytic conversion is much higher due to energy losses associated with the overpotentials required for the two chemical reactions and driving force for charge carrier transportation. Ultraviolet light (< 400 nm) only contributes less than 4% to sunlight spectrum, while 43% of light is in visible region (400~750 nm).

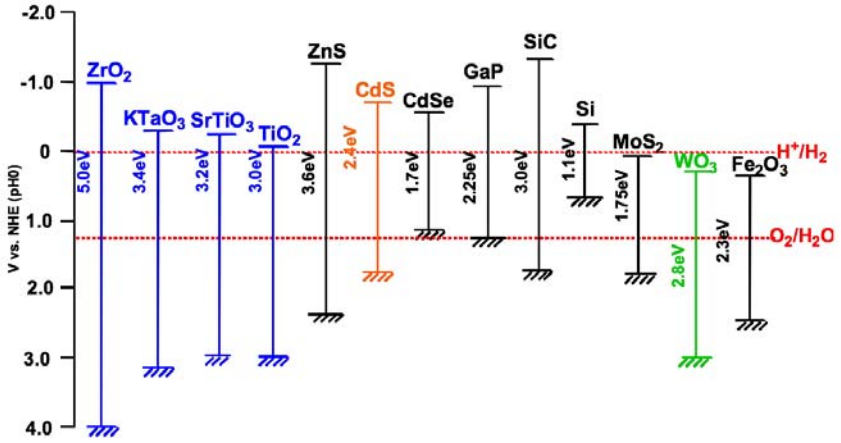

Fig. 2. Band levels of simple semiconductors. Reproduced from Ref. [12].

Therefore the development of a photocatalyst with activity from the UV through to visible wavelengths (~750 nm) and with a VB and CB that straddle the reaction potentials is one of key goals in obtaining optimum solar to fuel efficiency. The band gaps of some simple semiconductors have been measured and are shown in Fig. 2.

The reaction process on semiconductor photocatalysts is often considered as comprising three steps: (1) charge carrier (electron/hole) generation following absorption of a photon of suitable energy, (2) charge carrier separation and transportation, (3) chemical reaction between surface species and the charge carriers. The first two steps are photophysical and the final step is a chemical process. A photocatalytic reaction is therefore a complicated combination of photophysical and photochemical processes. Besides enhancing the ability of visible light harvesting (step (1)), there is equal importance in the development of a fast charge separation system (step (2)) and altering material morphology and surface modification to increase the reaction rate (step (3)).

There have been numerous examples in the literature of semiconductor materials that are able to evolve either hydrogen or oxygen from water in the presence of a suitable charge carrier scavenger (e.g. to have H_2 production, a hole scavenger is employed). However, the majority of these are unable to produce both oxygen and hydrogen simultaneously in stoichiometric ratio in the absence of sacrificial reagents. This demonstrates that although the correct positioning and energy of the band gap are prerequisite, it is not the sole factor in determining the heterogeneous photocatalytic activity. Other factors such as kinetic competition through charge carrier recombination, which may occur at a faster rate than the required surface reductive and oxidative chemistry, can be the dominant factor in determining reactivity towards the water splitting reaction.

In contrast to water splitting, only few examples have been reported for CO_2 photoconversion. Although CO_2 photoconversion has a similar mechanism, it requires 2–8 electrons to reduce CO_2 into the desired product. In other words, more free electrons are required in the photocatalyst. The difficulty for building up a high concentration of free electrons in the semiconductor is that the recombination rate would dramatically increase too.

2 Material development

2.1 Solar hydrogen generation

In 1972, Fujishima and Honda [16] found that TiO_2 can produce a photocurrent in an electrochemical cell when they used Pt as the counter-electrode and applied an electrical bias. Extensive research has been put into this field after this original benchmark was set. TiO_2 has been continually investigated by various methods, including doping with different elements, changing the particle morphology and applying different cocatalysts. In 1985, Yamaguti and Sato [17] found that Rh and NaOH co-loaded TiO_2 had an enormous increase in activity compared to TiO_2 itself in photocatalytic water splitting process. Selli et al. [18] reported electron transportation from TiO_2 photoanode to the Pt cathode was enhanced by a pH difference between the two under an external bias. Duonghong et al. [19] reported a TiO_2 colloid loaded with Pt and RuO_2 led to an increased quantum yield, and obtained both hydrogen and oxygen under UV illumination. H_2 generation rate reached 2.8 ml/h, which was much higher than the 1 ml/h without RuO_2 [20]. O_2 production was not detected at the beginning of the experiment, which was assumed due to its strong adsorption on the catalyst in the initial period. Instead of using anatase TiO_2, Fu et al. [21] studied bicrystalline titania (TiO_2(B)). They synthesised and investigated a heteropoly blue sensitizer and Pt loaded TiO_2(B) nanoribbon for water decompo-

sition for hydrogen evolution. Their result showed that a mixture of TiO_2(B) and anatase gave the maximum quantum yield (quantum yield (QY) = 8.11%), suggesting that interfacial charge separation improved the efficiency. In another report by this group, the solvent effect of water splitting was investigated. The hydrogen production rate was found to be increased in the presence of monochloroacetic acid and dichloroacetic acid with Pt/P25 as the photocatalyst [22]. A large number of investigations had made efforts to improve this cheap, stable, and non-toxic material. Unfortunately TiO_2 is still limited by its large band gap, which makes the photocatalyst only responsive to the UV or near UV region of the solar spectrum. Despite this, scientists have pioneered a range of UV responsive photocatalytic materials.

Domen's group paid particular attention to $SrTiO_3$ - a perovskite structured material [23–28]. They examined the use of a NiO cocatalyst mounted on $SrTiO_3$ as a photocatalyst in water under UV radiation, and reported both oxygen and hydrogen production. The study showed the NiO cocatalyst was prepared by H_2 reduction and subsequent O_2 oxidation on NiO to form a Ni/NiO_x double layer (termed NiO). Kim et al. [29] studied another important titanate, $La_2Ti_2O_7$, which is a layered structure material consisting of four TiO_6 unit slabs separated by La^{3+} ions layers. They reported that when $La_2Ti_2O_7$ splits water, H_2, and O_2 were produced in large amounts (QY up to 12%) in the presence of a NiO cocatalyst under UV. ZrO_2 has a very large band gap (5.0–5.7V), but can split water without a cocatalyst under UV illumination [30]. Sayama and Arakawa [31] reported the use of ZrO_2 with added alkali carbonate in water, $NaHCO_3$, gave the highest efficiency in water splitting. It is worth noting that the addition of other common metals and metal oxides as cocatalysts to ZrO_2 led to a decrease in photocatalytic activity in water splitting, which differed from other photocatalysts. This suggests that there is a large energetic barrier between the cocatalyst and semiconductor as a result of the large bandgap and position of the CB and VB. Jiang et al. [32] turned their attention to ZrW_2O_8 in order to overcome the problem of ZrO having large band gap. ZrW_2O_8 was estimated to have a band gap of about 4.0 eV. It showed ability to decompose water to yield hydrogen or oxygen in the presence of an appropriate electron or hole scavenger under a 300 W Hg-Xe lamp. The production rate wasn't particularly high, with 23.4 μmol/h of hydrogen and 9.8 μmol/h of oxygen [32].

Tantalates and niobates have shown high performances in photocatalytic activity for water splitting. Many researchers have studied and reported $MTaO_3$ [33–36], $M_2Ta_2O_7$ [37–39], MTa_2O_6 [40], and $M_2Nb_2O_7$ (M = alkaline metal or earth alkaline metal) [38,40,41] gave both hydrogen and oxygen production simultaneously when reacted with water under UV illumination. Although the large band gaps of these materials limit their ability to absorb the major parts of sunlight, the facile modification of the photocatalyst by the incorporation of a suitable foreign metal into the A/M or B sites in the perovskite structure (ABO_3) or tantalates/niobates allows the preparation of a different derivative photocatalyst. Kato et al. [34,35] reported NiO loaded $NaTaO_3$ exhibited a particularly high quantum yield (QY = 20% at 270 nm) for both hydrogen and oxygen production. In subsequent work [36], they found that by doping $NaTaO_3$/NiO with 2 mol% La, the quantum yield was increased dramatically to 56%. It was believed that the La ion had an effect in reducing the particle size and enhanced the material's surface area and reaction sites. $M_4Nb_6O_{17}$, a typical layered material, was active for complete water splitting under UV light as reported by Sayama [33]. In a further study it was suggested that H_2 and O_2 were produced in different layers, which reduced the chance of charge recombination. Although $M_4Nb_6O_{17}$ was able to split water without any cocatalyst, Domen reported that hydrogen production could be enhanced by suitable hole scavengers due to the ion exchange of protons [25].

Besides the transition metal photocatalysts, main group metal oxide materials have also been investigated as photocatalysts for water splitting by many researchers. Elements in groups 13 and 14, e.g. In, Sn, Sb, Ga, and Ge have been reported to be active for water splitting when mounted with appropriate cocatalysts. Sato et al. [42,43] reported MIn_2O_4 (M = Ca, Sr, and Ba), which had distorted InO_6 octahedra in the lattice, showed H_2 and O_2 production from pure water when a cocatalyst (RuO_x) was added to the materials through an impregnation method. $CaIn_2O_4$ exhibited the highest activity under UV light. Ye et al. [44–46] reported $MSnO_3$ (M = Ca, Sr, and Ba) suspended in pure water gave hydrogen and oxygen in the presence of a RuO_2 cocatalyst. $SrSnO_3$ had the highest photocatalytic activity due to a suitable band position and fast photogenerated charge carrier transfer in the proper distortion of SnO_6 in $SrSnO_3$. A study of the $SrSnO_3$ morphology found that $SrSnO_3$ nanorods achieved a 10 fold increase in photocatalytic activity when compared to standard particles with a similar surface area and optical density [46]. Sato et al. [47] have also found $M_2Sb_2O_7$ can split water into hydrogen and oxygen in a near-stoichiometric ratio under UV radiation.

A number of non-oxide materials such as sulphides and nitrides have been recognised for their ability to split water under UV illumination. The valence bands of these materials are composed of S 3*p* or N 2*p* orbitals. In this category, ZnS has been most investigated. Yanagida et al. [48] first reported the production of hydrogen from ZnS under 125 W Hg lamp illumination using tetrahydrofuran as hole scavenger. In another experiment, D_2O was used instead of water to confirm that the evolution of hydrogen was directly

caused by photocatalytic water splitting [48]. Reber et al. [49] systematically examined ZnS photocatalytic activity over a range of changing conditions including electron donor, pH and temperature. They reported a 90% quantum yield for hydrogen production at 313 nm illumination of ZnS coated with Pt in a solution of Na_2S, H_3PO_3, and NaOH [49,50]. Kobayakawa et al. [51] obtained hydrogen from $CuInS_2$ and $CuIn_5S_8$ suspended in water with a sulphite hole scavenger under UV illumination. However, all these metal sulphides or nitrides suffered from poor stability in the system, and they were easily oxidised by water.

Over 43% of sunlight is in the visible part of the spectrum, with only 4% of sunlight in UV region. In order to maximise the use of solar energy, the development of visible light driven photocatalysts is thus of the first priority. This means that the band gap of the material must be small. However, it is hard to find such a narrow band gap material with suitable CB and VB energy levels to provide the over-potentials for the redox reactions. WO_3 is a well-known photocatalyst for oxygen production in water oxidation, but the conduction band position of it makes hydrogen production energetically unfavourable. Attempts at incorporating different elements have been tried to enable hydrogen production on tungsten oxide to overcome the problem. $AgInW_2O_8$, $AgBiW_2O_8$, and Ag_2WO_4 were said to have a higher conduction band than WO_3 based on theoretical calculations, and which would allow hydrogen production. The latter material can actively produce both oxygen and hydrogen, as shown by Tang et al [52,53]. Kudo et al. [54–56] reported monoclinic $BiVO_4$, an important photocatalyst commonly used in water oxidation to produce oxygen, has a maximum QY of 9% under visible light (450nm) irradiation. It was found to be heavily dependent on the preparation method, and the crystal phase sample obtained from soft chemical synthesis with the monoclinic phase exhibited a higher activity than samples from high temperature solid reactions, regardless of the surface area of the catalyst. The lower efficiency was probably due to the higher number of defect sites in the material increasing the recombination probability.

Most of the visible light driven photocatalysts for water splitting require appropriate sacrificial reagents. Only a few metal oxides have been reported active for complete water splitting. Zou et al. [57] reported Ni-doped $InTaO_4$ can split water in absence of scavenger species. In the presence of a RuO_2 or NiO cocatalyst, the stoichiometric ratio of H_2 and O_2 was 2:1, with a QY of 0.66% at 402 nm. The undoped NiO-$InTaO_4$ has also been investigated and found to be less active, which was due to the replacement of Ni^{2+} to In^{3+} inducing a contraction of the lattice and the partially filled Ni *d*-orbitals reduced the band gap of the material leading to visible light absorption (< 480 nm).

Sulfides have also great potential as visible light photocatalysts for the production of solar H_2 but their application has been limited due to photo-corrosion. CdS has been the most extensively investigated due to its narrow band gap and ideal band positions for both O_2 and H_2 evolution (CB –0.87 eV and VB 1.5 eV vs. NHE). Both the Mills group [58] and Darwent group [59,60] studied CdS for H_2 production using EDTA as an electron donor. They found that with the addition of a Pt cocatalyst, CdS gave improved H_2 evolution rates by a factor of 10 from aqueous EDTA. A very high activity for H_2 evolution was reported for Pt-CdS in Na_2SO_3 aqueous solution (QY = 35%, 430 nm). Recently, Yan et al. [61] improved the activity of CdS for H_2 production in Na_2S and Na_2SO_3 solution by co-functionalizing CdS with Pt and PdS leading to a QY of 93% at 420 nm. Another report from Kalyanasundaram et al. [62] have shown that CdS with Pt and RuO_2 reduced the photocorrosion effect and gave an effective water splitting photocatalyst under visible light. In order to enhance the resistance to photocorrosion, electron donors such as S^{2-}, SO_3^{2-}, are often loaded into the water solution. Various strategies have been employed to overcome such problems, e.g., encapsulation of CdS nanoparticles, formation of CdS composites with TiO_2 and ZnS, and doping of CdS by noble metals and transition metals. Domen et al. [63–68] have developed a family of nitride/oxynitride visible light-driven materials. TaOH has been found to be active for O_2 evolution (QY = 34%, 420–500 nm) in the presence of $AgNO_3$ as electron scavenger [64]. More recently, systems comprising solid solutions of nitride-oxide mixtures were reported [69–71], such as GaN-ZnO, typically $Ga_{0.88}N_{0.88}Zn_{0.12}O_{0.12}$ coated with a cocatalyst $Rh_{2-x}Cr_xO_3$, which were able to split water with a high QY under visible illumination (QY = 5.9%, 420 nm). In order to get this record high QY, it was essential that the pH was adjusted to 4.5 with H_2SO_4.

Apart from the representative materials described above, others are described in several other important review works on materials for solar H_2 and/or O_2 production published recently. Those interested in these materials are recommended to read these reviews [11,12,72].

2.2 Photoreduction of CO_2

While photo-assisted water splitting has been heavily researched, CO_2 conversion has not yet been developed at the same rate. The reduction of CO_2 is a much more challenging process compared to water splitting, as 2–8 electrons are required to reduce CO_2 into potential hydrocarbon fuels. The significance of finding a suitable material that can do this is considered more important than hydrogen production, as it produces fuel and use CO_2 in one step, aiding both our energy needs and preventing increased climate change.

Reduction of CO_2 by a single crystal semiconducting material in a photoelectric system was reported by Halmann [73]. It was found that in an electrochemical cell, CO_2 can be reduced to give formic acid, formaldehyde, and methanol. The conditions were a single *p*-type GaP crystal as a photocathode, a carbon rod as the counter electrode, aqueous buffered electrolyte solution, and CO_2 bubbled through the solution, which were irradiated by a mercury lamp. In later work, the use of *p*-type GaAs and *p*-type InP single crystals to reduce CO_2 to methanol in CO_2-saturated Na_2SO_4 solution under bias was reported by Canfield and Frese [74].

The results published so far showed that semiconductor nanoparticles possess higher photocatalytic performance for CO_2 reduction compared to bulk material. Extremely small TiO_2 particles having large band gaps showed the highest efficiency for CH_4 formation [75]. Fujishima and Inoue et al. [76] first reported the photocatalytic reduction of CO_2 on various semiconductor powders, including GaP, TiO_2, ZnO, CdS, SiC, and WO_3, in an aqueous suspension system with CO_2 bubbling illuminated by a Xe lamp without of aid of an external bias. Overall, a small amount of formic acid, formaldehyde, methane, and methanol were produced. They suggested the conversion of CO_2 to hydrocarbon products occurred by a multistep reaction pathway, and the formation selectivity of product was influenced by the conduction band position of the photocatalyst. The yield of methanol increased as the conduction band of the photocatalysts became more negative compared to the redox potential of CH_3OH/H_2CO_3. WO_3 has a more positive conduction band than CH_3OH/H_2CO_3, and therefore methanol was not obtained in the process. Yahaya et al. [77] studied TiO_2, NiO and ZnO for CO_2 reduction under a 355 nm pulsed laser. From their result, they suggested that the reduction process of CO_2 does not follow a single mechanism, and the reduction of H_2CO_3 and carbonate ions as well as other mechanisms also affect the production of methanol.

TiO_2 has also drawn much interest in the CO_2 photocatalytic reduction research field, due to the suitability of its band gap as well as the aforementioned non-toxic, low-cost, and stable properties. There have been numerous modifications made on TiO_2. Anpo and Chiba [78] used dispersed TiO_2 anchored on porous Vycor glass to reduce CO_2 under UV illumination, which resulted in the production of methane, methanol, and carbon monoxide. From the direct detection of intermediate species, they proposed that methane came from the reaction between carbon radicals and atomic hydrogen. The photoreaction efficiency strongly depended on the CO_2 to H_2O ratio and reaction temperature.

Ichikawa and Doi [79] reduced CO_2 to methane and ethylene by Nafion film with TiO_2 and ZnO/Cu coated on different sides under an external bias, with 82% of the CO_2 converted, giving 44% of methane and 24% of ethylene. Their system consisted of a perforated thin film titania and an electrocatalyst separated by a proton separator. Water flowed into the thin film and CO_2 was passed through the photoelectrocatalyst. Sasirekha et al. [80] reported the photoreduction of CO_2 in water to produce methanol over Ru-doped TiO_2 on SiO_2. It was irradiated with a 1000 W high pressure mercury vapour lamp with a peak light intensity at 365 nm illumination. The ratio between Ru doping and TiO_2 was found to have an effect on the efficiency of the reaction. Enhancements of efficiency were achieved when 0.5% of Ru (200 μmol/g of methanol and methane from CO_2) or 10% of TiO_2 (250 μmol/g of methanol and methane from CO_2) was loaded with SiO_2. However, Ru-TiO_2/SiO_2 had a lower activity than TiO_2/SiO_2. The increase in efficiency was attributed to the UV transparent property of silica such that there was no loss of effectiveness of the UV irradiation on TiO_2, as was the case with bulk TiO_2 [81].

Xia et al. [82] reported the use of multiwalled carbon nanotubes blended with TiO_2 for CO_2 and water reduction. The selectivity of the product depended on the method used in material preparation: formic acid was obtained from hydrothermal synthesis and ethanol was produced from sol-gel synthesis. A recent research in the photocatalytic reduction of gas phase CO_2 by solar radiation was reported by Varghese and co-workers [83] using TiO_2 nanotube arrays with copper and Pt nanoparticles. Water vapour saturated carbon dioxide was reduced to methane and other hydrocarbons without an external bias. Various hydrocarbons were obtained at a production rate of 160 μl/(g·h) under AM 1.5 sunlight with loaded Cu and Pt.

Wu [84] reported methanol production (4.12 μmol/(g·h)) when a 1.0 wt% Ag/TiO_2 photocatalyst (coated around an optical fibre) was irradiated under a light intensity of 10 W/cm^2 in a specially designed reactor. An in situ FT-IR (Fourier transform infrared spectroscopy) study was carried out to investigate the mechanism of CO_2 reduction. The study proposed the reduction of CO_2 under UV irradiation occurred by a multistep mechanism, starting from the adsorption of linear CO_2. An electron and one hydrogen atom were added to yield products in the formate HCOO. Dioxymethylene (H_2COO) was then produced by adding another hydrogen atom. Dioxymethylene migrated to the oxygen vacancy on the TiO_2 site and accepted one electron and one oxygen atom was detached to form formaldehyde (H_2CO). Following this, methoxy (CH_3O) was formed from accepting another hydrogen atom. Finally, the methoxy reacted with water to give methanol [84]. In another report, NiO loaded $InTaO_4$ was examined in an optical fibre reactor. Methanol was yielded with production rate 11.3 μmol/(g·h) under concentrated sunlight and 11.1 μmol/(g·h) under 100 W halogen lamp [85].

Beside the developments made on TiO_2, several reports have been published on new photocatalytic materials for CO_2 reduction. After ZrO_2 was reported to be photocatalytically active for water splitting, Sayama and Arakawa [31] also found that ZrO_2 can reduce CO_2. They investigated the phenomena using a 1% Cu cocatalyst loaded-ZrO_2 as the photocatalyst in a $NaHCO_3$ solution (to provide the CO_2) under Hg lamp illumination. The reaction produced 19.5 mmol/h hydrogen, 10.8 mmol/h oxygen, and 2.5 mmol/h carbon monoxide. Lo et al. [86] have also investigated the use of ZrO_2 and P25 powder for CO_2 photoconversion using CO_2 mixed with H_2 and water under UV illumination. Carbon monoxide was produced as a sole product with ZrO_2, while with P25, methane, carbon monoxide, and ethene were obtained. Halmann et al. [76] examined CO_2 photoreduction by $SrTiO_3$ under sunlight in aqueous solution with CO_2 bubbling. Formic acid, formaldehyde, and methanol were produced as products. Matsumoto et al. [87] reported a *p*-type $CaFe_2O_4$ in sodium hydroxide solution under Hg lamp to convert CO_2, and obtained methanol and formaldehyde as the main product. Yan et al. [88] very recently reduced CO_2 by the UV driven material $ZnGa_2O_4$ in gaseous CO_2 with a small amount of water under a 300 W Xe lamp. Methane was detected under light irradiation. The production rate increased when mesoporous $ZnGa_2O_4$ was used instead of the bulk material. The methane production rate (4.8 μmol/(g·h)) increased 10 fold when the catalyst was loaded with 1 wt% RuO_2 as co-catalyst on mesoporous $ZnGa_2O_4$. Lately, $ZnGa_2O_4$ nanoribbon was also synthesized, which exhibited an even higher methane production rate under the same conditions. Methane production rate reached 25 μmol/(g·h) when 1% RuO_2 and 1% Pt were loaded [89].

Researchers have shown that increasing the dispersion of the photocatalysts had a positive effect on photoreactivity. Zeolite or silicate frameworks offer unique pore structures and ion exchange capacities; photocatalysts prepared within the zeolite cavity are highly dispersed. Anpo et al. [90] reported the reduction of CO_2 with water vapor by titania anchored on zeolite at 328 K under 75 W Hg lamp. It was found to have high selectivity for methanol formation. The addition of a Pt cocatalyst led to a shift in product selectivity: methane was obtained instead of methanol. In both reports, they emphasized that the TiO^{3+}-O^- charge transferred to the exited state of anchored titanium oxide played a significant role in determining photoactivity [78,90]. In another report, he reported Ti-containing porous SiO_2 film reduced CO_2 with water vapor gave CH_4 and CH_3OH with the quantum yield of 0.28% under Hg lamp radiation. They proposed a ligand-to-metal charge-transfer excitation of isolated Ti centers of framework-substituted micro or mesoporous silicates by UV light, which can be used to reduce CO_2 with H_2O at substantially better efficiency than the dense phase TiO_2 particles [91]. Ulagappam and Frei [92] reduced gaseous CO_2 by Ti silicate molecular sieves under 266 nm UV radiation to obtain formic acid, acetic acid, and CO. FT-IR studies of the reaction showed that formation of CO was produced by the photolysis of formic acid, and acetic acid were synthesised from the Tischenko reaction of formaldehyde [92]. Lin and co-workers [93] studied the reduction of CO_2 and water vapour/D_2O vapour by TiMCM-41 molecular sieve under laser light. Carbon monoxide was the only product in the reaction, and the production rate was directly proportional to the power of the laser. FT-IR data showed that formation of CO was due to the double electron transfer of CO_2. In Lin and Frei's work [94], CO_2 was reduced by ZrCu(I)-MCM-41 silicate sieve under 355 nm UV irradiation to give CO and O_2.

While several new oxide photocatalysts were being developed, the process of photoreduction by metallic complex catalysts, such as ruthenium complexes, has also drawn equal interest. Takeda et al. [95] reported the reduction of CO_2 by a rhenium complex in DMF solution to give CO. Lehn and Ziessel [96] investigated the use of Ru(2,2'-bipyridine)$_3^{2+}$ cobalt (II) chloride in a mixture of $CH_3CN/H_2O/N(CH_2CH_3)_3$ to reduce CO_2 under visible light illumination. Craig et al. [97] reported CO_2 can be reduced by Ru(bpy)$^{+}$ with a Ni complex cocatalyst in an adsorbate buffered solution to give CO. There is serious concern of cost and stability of these noble metal-based complex photocatalysts in aqueous solution. Fujita [98] has summarised the early developments in this field using different metal complexes.

In the majority of these reports, no concurrent O_2 production was reported and most CO_2 reduction reactions were achieved in an electrochemical cell requiring UV illumination and/or an electrical bias. The maximum conversion of CO_2 was at the micromole level per hour. The efficiency of this process is therefore extremely low at this stage and the details of the mechanism of this reaction have yet to be clarified, which lags considerably behind solar hydrogen research. However the potential of the field is huge: this technology can provide the best solution to decrease CO_2 emission and the desired products are compatible with present fuel transportation and storage systems, which thus can be used directly by users. For future development, more efficient materials and structure need to be found. Given the importance of the mechanism underlying CO_2 photoconversion, it has hardly been addressed and should be paid more attention in the future. For more on CO_2 conversion, the very recent report of Roy et al. [13] is recommended, which discussed the conversion of CO_2 with different strategies including biomass, thermochemical, electrochemical and photochemical conversions. Usubharatana et al. [14] have

also summarized the progress of photocatalyst development, concentrating on the design of the photoreactor, effect of CO_2 concentration and reaction temperature.

3 Key factors in determining photocatalyst activity

3.1 Particle size of photocatalyst

The particle size of a photocatalyst has a direct effect on the photocatalytic reactivity. The change in reactivity may be caused by several factors as follows. (1) Total surface area per volume of the photocatalyst increases. It is expected that the surface area has a direct effect on the photocatalytic activity. The increase in surface area provides more reaction sites. (2) The particle size has a significant effect on initial charge carrier transportation and separation and thus on the rate of electron-hole recombination. For example, in the study on $NaNbO_3$ samples, an increase from 1.7 m^2/g to 38 m^2/g in surface area by changing the synthesis method led to a tripling in O_2 evolution rate and the H_2 production rate increased six fold [99]. (3) Several theoretical results have been published showing that the particle size of the semiconductor nanoparticle has a direct effect on the semiconductor bandgap [100–104]. A decrease in particle size resulted in an enlargement of the bandgap of the photocatalyst, consequently both oxidising and reduction power became stronger [104].

3.2 Choice of cocatalyst

Cocatalysts have been shown to be very important and to some extent crucial in determining the activity of a system. For photochemical water splitting, cocatalysts such as NiO, RuO_2, Pt, and $Rh_{2-x}Cr_xO_3$ are often employed. NiO has been very widely used to achieve stoichiometric hydrogen and oxygen production from water [28]. The effects of cocatalysts are clearly shown on the two most active materials for photocatalytic water splitting under visible light. The NiO/Ni shell/core structure is the key factor in the activity of $In_{0.9}Ni_{0.1}TaO_4$ [57], whilst $Ga_{0.88}N_{0.88}Zn_{0.12}O_{0.12}$ does not show any activity for water splitting in the absence of $Rh_{2-x}Cr_xO_3$. Currently the exact mechanisms of enhancement of activity are not known for most cocatalysts, which complicates the choice of the appropriate material. The water splitting performance of Zn_2GeO_4 was found to increase by mounting the system with Pt and RuO_2. The photocatalytic activity of Pt-RuO_2/Zn_2GeO_4 markedly increased from 4.0 to 53.4 μmol/h for hydrogen production and 2.0 to 26.0 μmol/h for oxygen production [105].

Liu et al. [67] reported $Y_2Ta_2O_5N_2$ photoactivity was promoted by the deposition of metal Pt and Ru, and the maximum hydrogen evolution rate (833 μmol/(h·g) was found with 0.15 wt% Pt and 0.25 wt% Ru coated on $Y_2Ta_2O_5N_2$, which was 22 times more than that for 0.15 wt% Pt/$Y_2Ta_2O_5N_2$. Recently, Maeda et al. [106] reported for the first time the possibility of enhancing overall water splitting by the addition of both core/shell-structured Rh/Cr_2O_3 and Mn_3O_4 nanoparticles as H_2 and O_2 evolution promoters onto the same photocatalyst.

For CO_2 conversion, there are also a few examples that showed the addition of a cocatalyst led to an increase in catalytic performance and can change the end product of the reaction. The photocatalytic performance of TiO_2 was improved by the addition of a Cu cocatalyst [107]. Cook and co-workers [108] reported the reduction of CO_2 by SiC to different hydrocarbons (CH_4, C_2H_4, and C_2H_6) as a function of electrolyte pH. SiC performance was enhanced by loading a Cu cocatalyst, showing that Cu particles enhanced the reduction of CO_2. In another experiment, a gaseous water and CO_2 mixture was reduced by TiO_2-SiO_2-acetylacetone (ACAC) under UVA radiation. Methane was obtained from pure TiO_2-SiO_2-ACAC, whereas in the presence of 0.5 wt% Cu and 0.5 wt% Fe cocatalysts, both methane and ethylene were detected [84].

3.3 Other factors

The crystal structure and morphology of the photocatalyst also play an important role in influencing the photocatalytic performance. Ye et al. [44–46] found that $SrSnO_3$ prepared by two different methods showed significantly different activity: $SrSnO_3$ consists of sphere-like particles when synthesized by a solid state reaction while the other sample was a nano-rod structure when prepared by hydrothermal synthesis. Both materials had a similar optical absorption and surface area, but the photocatalytic activity was found to be 10 times higher with the nano-rod structure.

A similar phenomenon was also observed on TiO_2, and a correlation between the surface phases of TiO_2 and its photocatalytic performance was investigated by Zhang et al. [109]. The photocatalytic activity of TiO_2 was found to increase dramatically when anatase TiO_2 particles were deposited on the surface of a rutile TiO_2 bulk. The phenomenon was suggested to be caused by a surface-phase junction to facilitate the charge separation, which in turn increased the photogenerated hole-electron lifetime. This led to the increase in photocatalytic activity.

The effect of La doping of $NaTaO_3$ was reviewed and the presence of the dopant led to a nanostructuring effect that was proposed to be a key factor in a large enhancement in photocatalytic activity [36,110]. $LiTaO_3$ and $KTaO_3$ consist of corner-shared TaO_6 octahedra. Their ability at splitting water was investigated and it was found the closer the bond

angle of Ta–O–Ta was to 180°, the better the charge separation and the smaller the band gap. Upon changing the alkali metal, $LiTaO_3$, $NaTaO_3$, $KTaO_3$ have Ta–O–Ta angles of 143°, 163°, and 180°, respectively. This was reported to enhance electron-hole migration through the crystal ($LiTaO_3$ < $NaTaO_3$ < $KTaO_3$) which had an effect on the photocatalytic activity, as shown in Table 1 [33–35].

Table 1 Photoactivity of different alkali metal tantalates for water splitting [33–35]

Catalyst	Band gap (eV)	Activity (mol/h)	
		H_2	O_2
$LiTaO_3$	4.7	6	2
$NaTaO_3$	4.0	4	1
$KTaO_3$	3.6	29	13

The effects of the condition of stabilizers used on semiconductor materials for CO_2 conversion have also been investigated. $Cd(ClO_4)_2$ and different types of polymers were mixed to prepared CdS. A different polymer used led to a different product. A negatively charged stabilizer favoured the photoreduction of CO_2 to formate, while CO was more easily produced with a positively charged polymer under Xe lamp radiation [104,111].

4 Mechanism of photocatalytic synthesis

An estimate states that the minimum requirement of 10% conversion efficiency is required for light driven photocatalytic hydrogen production to become commercially viable [112]. Currently, no reported material has met this requirement in prolonged periods of use.

The solar energy conversion efficiency is assumed to be below 1% in the above researches although the authors did not report the conversion efficiency but the quantum yield [71]. Knowing the mechanism of the photocatalytic process would help the development of new materials in this field. However, very little effort has been put into mechanistic research, with only a few reports on the fundamental mechanisms of water splitting and CO_2 photoreduction being published.

As mentioned above, there are three basic processes in semiconductor photocatalysis. In addition to extending the absorption profile of materials to harvest a greater portion of the solar spectrum by narrowing the band width of the material, minimizing the loss of electrons and holes excited by photons is equally important. Fundamental researches have mainly focused on the charge carrier separation and transportation. It is believed that a faster charger carrier separation rate leads to an increase in charges lifetime. Transient absorption spectroscopy (TAS) is a powerful technique to monitor the dynamics and life time of charge carriers. It is an extension of absorption spectroscopy. The absorbance of charge carriers at a particular wavelength or range of wavelengths in a sample is measured as a function of time after excitation by a flash of light. The pulse of light for excitation is generated by a laser and the light for measuring the absorbance can be either a laser or a CW lamp equipped with a monochrometer.

The behaviour of charge carriers in TiO_2 has been investigated by TAS measurement following initial UV laser excitation of TiO_2 colloids and nanocrystalline TiO_2 films. The initial trapping time and further relaxation time have been reported as occurring within 200 fs and 500 ps, respectively [113]. Tang et al. and other groups reported the TAS of the trapped photoelectrons and holes in nc-TiO_2, with a maximum absorption of holes at 450 nm and electrons at 800 nm upward [114–116].

The electron-hole decay time has been reported to be in a range of different rates with changing particle size. It was found that complete electron hole recombination occurred in 10 ns in 2.1 nm diameter TiO_2 whereas only 90% of the charge carriers recombined within 10 ns in 13.3 nm and 26.7 nm TiO_2 colloidal particle [117]. Several TAS studies have proposed the UV excitation intensity has an effect on the rate of recombination. Under light intensities that are close to solar radiation intensities, power law type decays beyond the microsecond timescale have been observed [113,116,118]. This fast electron-hole recombination was believed to be the main reason behind the lack of water splitting activity of nc-TiO_2 without a cocatalyst or chemical scavenger. Tang et al. [116] reported that in the presence of a silver (Ag^+) electron-scavenger, the reaction rate between Ag^+ and the electron was very fast, leaving holes to react with water to produce O_2 (Fig. 3(1) and (4)). O_2 production has been estimated to require an average hole lifetime of

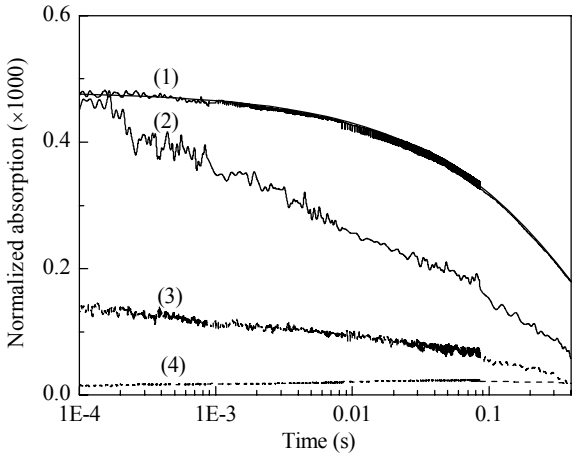

Fig. 3. Dynamics of holes (traces (1) and (2)) and electrons (traces (3 and (4)) in TiO_2 film with Ag^+ (traces (1) and (4)) and Pt (traces (2) and (3)) as the electron scavengers after bandgap excitation with laser wavelength of 335 nm. Figure reproduced from Ref. [116].

~0.2 s at a neutral pH. The observed rate of decay of the holes on nc-TiO_2 consisted of several components as water oxidation is a multi-step reaction. It has been suggested that four holes are required to oxidize water to produce one oxygen molecule in artificial water splitting systems. Later, they experimentally observed and proved the 4-hole chemistry in artificial water splitting systems [116]. In Fig. 4, an nc-TiO_2 water splitting process is summarized to illustrate the key reaction timescales, which was based on a range of TAS studies [116,117,119].

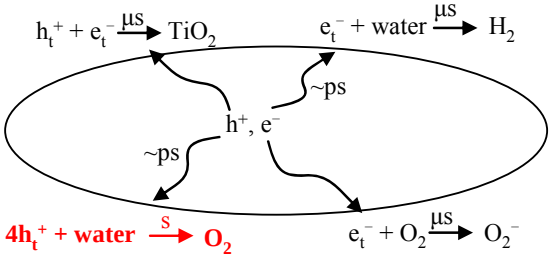

Fig. 4. Timescales of processes occurring on nc-TiO_2 following UV excitation. Figure reproduced from Ref. [116].

TAS measurements have also been studied on TiO_2 co-doped with both Sb and Cr and several other materials closely related to nc-TiO_2. These photocatalysts show oxygen production under visible light in the presence of Ag^+ as a scavenger. The maximum oxygen yield has been found to occur when TiO_2 was doped with Cr and Sb in a 1:2 ratio, due to an increased charge carriers lifetime [120]. The electron hole dynamics on a range of materials including TiO_2 hybrids and doped TiO_2 samples has also been examined by the two groups of Majima's and Tang's. The previously mentioned alkali metal tantalates have been examined by Tachikawa et al. [121]. Besides restructuring the nano-morphology of $NaTaO_3$, La doping leads to greatly reduced recombination in TAS measurements [122]. Tang et al. [123] recently reported the low efficiency of the nitrogen doped TiO_2 was mainly due to the newly-generated trapped sites of electrons.

As discussed above, CO_2 photoreduction has received much less attention than solar hydrogen production. Although the knowledge is known to be important for enhancing material efficiency, there are few studies on the mechanism of CO_2 photoreduction. Nevertheless, the process of CO_2 reduction shares an approximately similar mechanism with solar water splitting. Experiences gained from water splitting may also be applied to CO_2 photoreduction.

5 Conclusions

Directly utilizing solar energy will provide future generations with a sustainable power source and a clean environment. However, the storage of solar energy has been a major problem in the field. The ideal solution is to convert solar energy into readily transportable and highly energetic chemicals, e.g. hydrogen or hydrocarbon fuels. The benefits of photocatalytic water splitting or CO_2 conversion will truly be realized when accompanied by an effective hydrogen/methanol fuel cell/engine to utilize the fuels and oxygen produced from a photocatalytic system to generate power and water, giving us a carbon free or carbon neutral cycle.

During the past 30 years, many efforts have been made towards the development of materials and systems to convert water to O_2 and H_2 together in a water splitting process, or to convert CO_2 to hydrocarbon fuels. Unfortunately, to date there is no material or device that has the required conversion efficiency to make this technology economically and commercially viable. The key factors which have been reported including band positions of the conduction and valence bands, the choice of cocatalyst, the morphology and particle size, are aspects of the field which must be pursued. Fundamental research on exploring how electrons and holes move and react in each photocatalyst will give a better understanding of the factors that control photocatalytic activity. This has not been clearly identified and should be addressed systematically for an efficient photochemical process.

Acknowledgments

Funding from EPSRC on Solutions is gratefully acknowledged.

References

1 Hoffert M I, Caldeira K, Jain A K, Haites E F, Harvey L D D, Potter S D, Schlesinger M E, Schneider S H, Watts R G, Wigley T M L, Wuebbles D J. *Nature*, 1998, **395**: 881
2 Lewis N S, Nocera D G. *Proc Natl Acad Sci USA*, 2006, **103**: 15729
3 Energy Information Administration. Annual Energy Review 2008. Washington DC: U.S. Department of Energy, 2009
4 Barber J. *Chem Soc Rev*, 2009, **38**: 185
5 Hansen J E. *Environmental Research Letters*, 2007, **2**: 024002
6 Hansen J E, Sato M, Kharecha P, Beerling D, Berner R, Masson-Delmotte V, Pagani M, Raymo M, Royer D L, Zachos J C. *The Open Atmospheric Science Journal*, 2008, **2**: 217
7 Http://fossil.energy.gov/sequestration/geologic/index.html, U.S. Department of Energy, 2010
8 Halbwachs M, Sabroux J C. *Science*, 2001, **292**: 438
9 Chisti Y. *Biotechnol Adv*, 2007, **25**: 294
10 Sharma Y C, Singh B, Upadhyay S N. *Fuel*, 2008, **87**: 2355
11 Tang J W, Cowan A. In: Griesbeck A, Oelgemoeller M, Ghetti F, eds. CRC Handbook of Organic Photochemistry & Photo-

biology. 3rd Ed. London: CRC Press, 2012
12 Kudo A, Miseki Y. *Chem Soc Rev*, 2009, **38**: 253
13 Roy S C, Varghese O K, Paulose M, Grimes C A. *ACS Nano*, 2010, **4**: 1259
14 Usubharatana P, McMartin D, Veawab A, Tontiwachwuthikul P. *Ind Eng Chem Res*, 2006, **45**: 2558
15 Centi G, Perathoner S. *ChemSusChem*, 2010, **3**: 195
16 Fujishima A, Honda K. *Nature*, 1972, **238**: 37
17 Yamaguti K, Sato S. *J Chem Soc*, *Faraday Trans I*, 1985, **81**: 1237
18 Selli E, Chiarello G L, Quartarone E, Mustarelli P, Rossetti I, Forni L. *Chem Commun*, 2007: 5022
19 Duonghong D, Borgarello E, Gratzel M. *J Am Chem Soc*, 1981, **103**: 4685
20 Sato S, White J M. *Chem Phys Lett*, 1980, **72**: 83
21 Fu N, Wu Y, Jin Z, Lu G. *Langmuir*, 2010, **26**: 447
22 Li Y X, Me Y Z, Peng S Q, Lu G X, Li S B. *Chemosphere*, 2006, **63**: 1312
23 Domen K, Kudo A, Onishi T. *J Catal*, 1986, **102**: 92
24 Domen K, Kudo A, Onishi T, Kosugi N, Kuroda H. *J Phys Chem*, 1986, **90**: 292
25 Domen K, Kudo A, Shibata M, Tanaka A, Maruya K, Onishi T. *Chem Commun*, 1986: 1706
26 Domen K, Naito S, Onishi T, Tamaru K, Samo M. *Chem Phys Lett*, 1982, **92**: 433
27 Domen K, Naito S, Onishi T, Tamaru K, Samo M. *J Phys Chem*, 1982, **86**: 3657
28 Domen K, Naito S, Soma M, Onishi T, Tamaru K. *Chem Commun*, 1980: 543
29 Kim J, Hwang D W, Kim H G, Bae S W, Lee J S, Li W, Oh S H. *Top Catal*, 2005, **35**: 295
30 Chang S M, Doong R A. *J Phys Chem B*, 2004, **108**: 18098
31 Sayama K, Arakawa H. *J Phys Chem*, 1993, **97**: 531
32 Jiang L, Wang Q Z, Li C L, Yuan J A, Shangguan W F. *Int J Hydrogen Energy*, 2010, **35**: 7043
33 Sayama K, Arakawa H, Domen K. *Catal Today*, 1996, **28**: 175
34 Kato H, Kudo A. *Chem Phys Lett*, 1998, **295**: 487
35 Kato H, Kudo A. *J Phys Chem B*, 2001, **105**: 4285
36 Kato H, Asakura K, Kudo A. *J Am Chem Soc*, 2003, **125**: 3082
37 Mitsui C, Nishiguchi H, Fukamachi K, Ishihara T, Takita Y. *Chem Lett*, 1999, 1327
38 Ikeda S, Fubuki M, Takahara Y K, Matsumura M. *Appl Catal A*, 2006, **300**: 186
39 Kudo A, Kato H, Nakagawa S. *J Phys Chem B*, 2000, **104**: 571
40 Kato H, Kudo A. *Chem Lett*, 1999, 1207
41 Yoshino M, Kakihana M, Cho W S, Kato H, Kudo A. *Chem Mater*, 2002, **14**: 3369
42 Sato J, Kobayashi H, Inoue Y. *J Phys Chem B*, 2003, **107**: 7970
43 Sato J, Kobayashi H, Saito N, Nishiyama H, Inoue Y. *J Photochem Photobiol A*, 2003, **158**: 139
44 Zhang W F, Tang J W, Ye J H. *Chem Phys Lett*, 2006, **418**: 174
45 Zhang W F, Tang J W, Ye J H. *J Mater Res*, 2007, **22**: 1859
46 Chen D, Ye J H. *Chem Mater*, 2007, **19**: 4585
47 Sato J, Saito N, Nishiyama H, Inoue Y. *J Photochem Photobiol A*, 2002, **148**: 85
48 Yanagida S, Azuma T, Sakurai H. *Chem Lett*, 1982: 1069
49 Reber J F, Meier K. *J Phys Chem*, 1984, **88**: 5903
50 Wu M, Gu W Z, Li W Z, Zhu X W, Wang F D, Zhao S T. *Sci Technol Catal*, 1995, **92**: 257
51 Kobayakawa K, Teranishi A, Tsurumaki T, Sato Y, Fujishima A. *Electrochim Acta*, 1992, **37**: 465
52 Tang J W, Ye J H. *J Mater Chem*, 2005, **15**: 4246
53 Tang J W, Zou Z G, Ye J H. *J Phys Chem B*, 2003, **107**: 14265
54 Kudo A, Omori K, Kato H. *J Am Chem Soc*, 1999, **121**: 11459
55 Kudo A, Ueda K, Kato H, Mikami I. *Catal Lett*, 1998, **53**: 229
56 Yu J Q, Kudo A. *Adv Funct Mater*, 2006, **16**: 2163
57 Zou Z G, Ye J H, Sayama K, Arakawa H. *Nature*, 2001, **414**: 625
58 Mills A, Porter G. *J Chem Soc*, *Faraday Trans I*, 1982, **78**: 3659
59 Darwent J R. *J Chem Soc*, *Faraday Trans II*, 1981, **77**: 1703
60 Darwent J R, Porter G. *Chem Commun*, 1981: 145
61 Yan H J, Yang J H, Ma G J, Wu G P, Zong X, Lei Z B, Shi J Y, Li C. *J Catal*, 2009, **266**: 165
62 Kalyanasundaram K, Borgarello E, Duonghong D, Gratzel M. *Angew Chem*, *Int Ed*, 1981, **20**: 987
63 Hara M, Hitoki G, Takata T, Kondo J N, Kobayashi H, Domen K. *Catal Today*, 2003, **78**: 555
64 Hara M, Nunoshige J, Takata T, Kondo J N, Domen K. *Chem Commun*, 2003: 3000
65 Takata T, Hitoki G, Kondo J N, Hara M, Kobayashi H, Domen K. *Res Chem Intermed*, 2007, **33**: 13
66 Yamasita D, Takata T, Hara M, Kondo J N, Domen K. *Solid State Ionics*, 2004, **172**: 591
67 Liu M Y, You W S, Lei Z B, Zhou G H, Yang J J, Wu G P, Ma G J, Luan G Y, Takata T, Hara M, Domen K, Li C. *Chem Commun*, 2004: 2192
68 Hitoki G, Takata T, Kondo J N, Hara M, Kobayashi H, Domen K. *Electrochemistry*, 2002, **70**: 463
69 Maeda K, Takata T, Hara M, Saito N, Inoue Y, Kobayashi H, Domen K. *J Am Chem Soc*, 2005, **127**: 8286
70 Maeda K, Teramura K, Domen K. *J Catal*, 2008, **254**: 198
71 Maeda K, Teramura K, Lu D L, Takata T, Saito N, Inoue Y, Domen K. *Nature*, 2006, **440**: 295
72 Osterloh F E. *Chem Mater*, 2008, **20**: 35
73 Halmann M. *Nature*, 1978, **275**: 115
74 Canfield D, Frese K W. *J Electrochem Soc*, 1983, **130**: 1772
75 Yamashita H, Nishiguchi H, Kamada N, Anpo M, Teraoka Y, Hatano H, Ehara S, Kikui K, Palmisano L, Sclafani A, Schiavello M, Fox M A. *Res Chem Intermed*, 1994, **20**: 815
76 Inoue T, Fujishima A, Konishi S, Honda K. *Nature*, 1979, **277**: 429
77 Yahaya A H, Gondal M A, Hameed A. *Chem Phys Lett*, 2004, **400**: 206
78 Anpo M, Chiba K. *J Mol Catal*, 1992, **74**: 207
79 Ichikawa S, Doi R. *Catal Today*, 1996, **27**: 271
80 Sasirekha N, Basha S J S, Shanthi K. *Appl Catal B*, 2006, **62**: 169

81 Matthews R W. *J Catal*, 1988, **113**: 549
82 Xia X H, Jia Z H, Yu Y, Liang Y, Wang Z, Ma L L. *Carbon*, 2007, **45**: 717
83 Varghese O K, Paulose M, LaTempa T J, Grimes C A. *Nano Lett*, 2009, **9**: 731
84 Wu J C S. *Catal Surveys Asia*, 2009, **13**: 30
85 Wang Z Y, Chou H C, Wu J C S, Tsai D P, Mul G. *Appl Catal A*, 2010, **380**: 172
86 Lo C C, Hung C H, Yuan C S, Wu J F. *Sol Energy Mater Sol Cells*, 2007, **91**: 1765
87 Matsumoto Y, Obata M, Hombo J. *J Phys Chem*, 1994, **98**: 2950
88 Yan S C, Ouyang S X, Gao J, Yang M, Feng J Y, Fan X X, Wan L J, Li Z S, Ye J H, Zhou Y, Zou Z G. *Angew Chem*, *Int Ed*, 2010, **49**: 6400
89 Liu Q, Zhou Y, Kou J H, Chen X Y, Tian Z P, Gao J, Yan S C, Zou Z G. *J Am Chem Soc*, 2010, **132**: 14385
90 Anpo M, Yamashita H, Ichihashi Y, Fujii Y, Honda M. *J Phys Chem B*, 1997, **101**: 2632
91 Ikeue K, Nozaki S, Ogawa M, Anpo M. *Catal Lett*, 2002, **80**: 111
92 Ulagappan N, Frei H. *J Phys Chem A*, 2000, **104**: 7834
93 Lin W Y, Han H X, Frei H. *J Phys Chem B*, 2004, **108**: 18269
94 Lin W Y, Frei H. *J Am Chem Soc*, 2005, **127**: 1610
95 Takeda H, Koike K, Inoue H, Ishitani O. *J Am Chem Soc*, 2008, **130**: 2023
96 Lehn J M, Ziessel R. *Proc Natl Acad Sci USA*, 1982, **79**: 701
97 Craig C A, Spreer L O, Otvos J W, Calvin M. *J Phys Chem*, 1990, **94**: 7957
98 Fujita E. *Coord Chem Rev*, 1999, **185-186**: 373
99 Li G Q, Kako T, Wang D F, Zou Z G, Ye J H. *J Phys Chem Solids*, 2008, **69**: 2487
100 Brus L E. *J Chem Phys*, 1984, **80**: 4403
101 Lippens P E, Lannoo M. *Phys Rev B*, 1989, **39**: 10935
102 Wang Y, Suna A, Mahler W, Kasowski R. *J Chem Phys*, 1987, **87**: 7315
103 Henglein A. *Chem Rev*, 1989, **89**: 1861
104 Yoneyama H. *Catal Today*, 1997, **39**: 169
105 Ma B J, Wen F Y, Jiang H F, Yang J H, Ying P L, Li C. *Catal Lett*, 2010, **134**: 78
106 Maeda K, Xiong A K, Yoshinaga T, Ikeda T, Sakamoto N, Hisatomi T, Takashima M, Lu D L, Kanehara M, Setoyama T, Teranishi T, Domen K. *Angew Chem*, *Int Ed*, 2010, **49**: 4096
107 Adachi K, Ohta K, Mizuno T. *Solar Energy*, 1994, **53**: 187
108 Cook R L, Macduff R C, Sammells A F. *J Electrochem Soc*, 1988, **135**: 3069
109 Zhang J, Xu Q, Feng Z, Li M, Li C. *Angew Chem*, *Int Ed*, 2008, **47**: 1766
110 Kudo A, Kato H. *Chem Phys Lett*, 2000, **331**: 373
111 Inoue H, Nakamura R, Yoneyama H. *Chem Lett*, 1994: 1227
112 Bard A J, Fox M A. *Acc Chem Res*, 1995, **28**: 141
113 Tamaki Y, Furube A, Murai M, Hara K, Katoh R, Tachiya M. *Phys Chem Chem Phys*, 2007, **9**: 1453
114 Yoshihara T, Katoh R, Furube A, Tamaki Y, Murai M, Hara K, Murata S, Arakawa H, Tachiya M. *J Phys Chem B*, 2004, **108**: 3817
115 Bahnemann D, Henglein A, Lilie J, Spanhel L. *J Phys Chem*, 1984, **88**: 709
116 Tang J W, Durrant J R, Klug D R. *J Am Chem Soc*, 2008, **130**: 13885
117 Serpone N, Lawless D, Khairutdinov R. *J Phys Chem*, 1995, **99**: 16646
118 Murai M, Tamaki Y, Furube A, Hara K, Katoh R. *Catal Today*, 2007, **120**: 214
119 Yamakata A, Ishibashi T, Onishi H. *J Phys Chem B*, 2001, **105**: 7258
120 Ikeda T, Nomoto T, Eda K, Mizutani Y, Kato H, Kudo A, Onishi H. *J Phys Chem C*, 2008, **112**: 1167
121 Tachikawa T, Fujitsuka M, Majima T. *J Phys Chem C*, 2007, **111**: 5259
122 Yamakata A, Ishibashi T, Kato H, Kudo A, Onishi H. *J Phys Chem B*, 2003, **107**: 14383
123 Tang J W, Cowan A, Durrant J R, Klug D R. *J Phys Chem C*, 2011, **115**: 3143